

Junctophilin-2 uses S-palmitoylation to reinforce its role as a junctional sarcoplasmic reticulum-plasma membrane tether

Min Jiang, Junping Hu, Frances K. H. White, Judy Williamson,
Andrey S. Klymchenko, Akshay Murthy, Samuel W. Workman, and Gea-Ny Tseng

List of material included

- A. Supplemental figures
- B. Supplemental references
- C. Sequence alignment of human and rat JPH2
- D. Sequence alignment among human JPH1-JPH4
- E. Ranking of potential S-palmitoylation sites in JPH1-JPH4 using CSS-Palm 4.0

A. SUPPLEMENTAL FIGURES

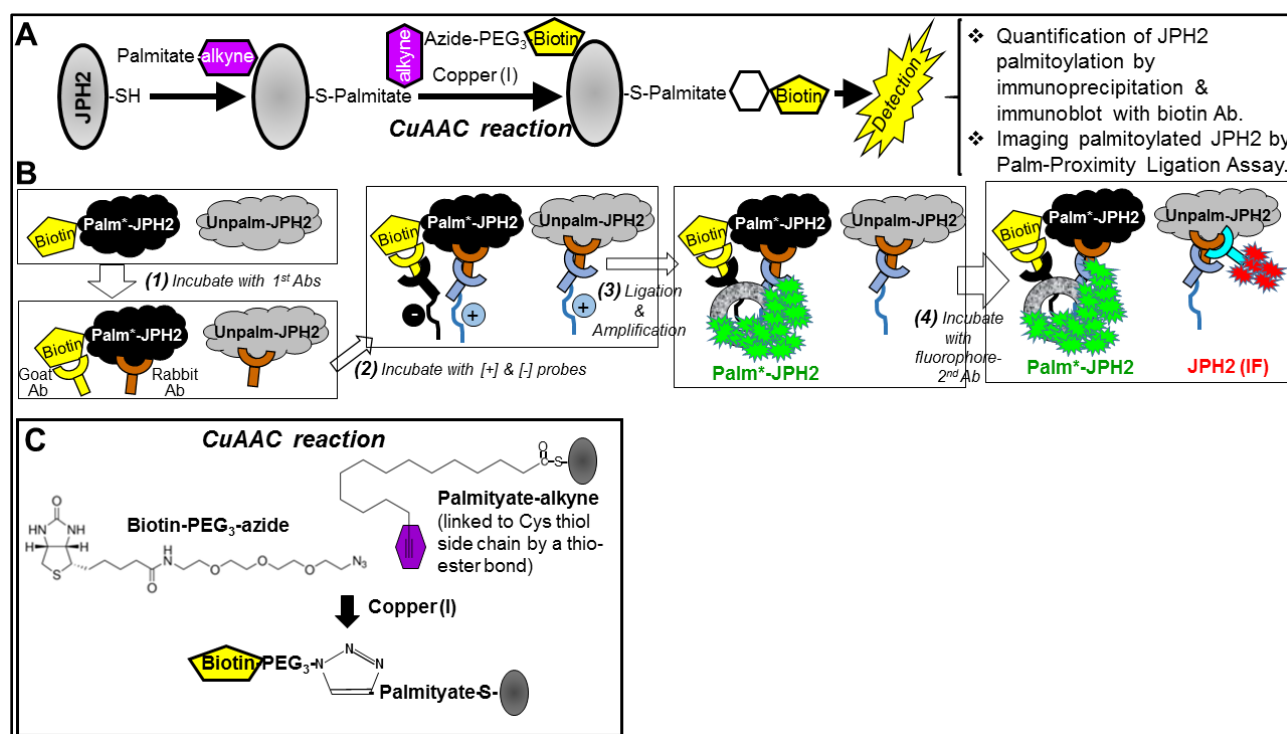


Fig. S1 Experimental procedures to quantify JPH2 palmitoylation and to monitor its distribution in cells. (A) Cells expressing JPH2 were incubated with palmitate-alkyne to allow linkage of palmitate-alkyne to cysteine thiols in S-palmitoylation reaction. Cu(I)-catalyzed azide-alkyne cycloaddition, ‘CuAAC reaction’, was performed in the presence of biotin-PEG₃-azide to biotinylate palmitoylated proteins. This allowed biotin Ab-based detection/quantification of palmitoylated JPH2 (Palm^{*}-JPH2). **(B)** Using in situ Proximity Ligation Amplification (PLA) to detect palmitoylated JPH2. Palmitoylated JPH2 was biotinylated in the CuAAC reaction with biotin-PEG₃-azide, followed by four major steps: (1) incubation with primary antibodies (1st Abs) targeting biotin and JPH2 (e.g. biotin goat Ab and JPH2 rabbit Ab), (2) incubation with [+] and [-] probes, which were secondary Abs conjugated with complementary oligonucleotides that targeted goat Ab and rabbit Ab respectively, (3) oligonucleotide-ligation reaction followed by rolling circle amplification reaction producing a bundle of ~ 100 kb DNA strand labeled with several hundred fluorophores at each of the proximity ligation sites¹, (4) JPH2 that were not labeled by the proximity ligation amplification product were labeled by immunofluorescence, JPH2 (IF), i.e. Alexa fluorophore-conjugated secondary (2nd) Ab targeting JPH2 rabbit Ab. In this example, PLA signals were detected by green fluorophore and JPH2 (IF) was detected by red fluorophore. **(C)** details of CuAAC reaction.

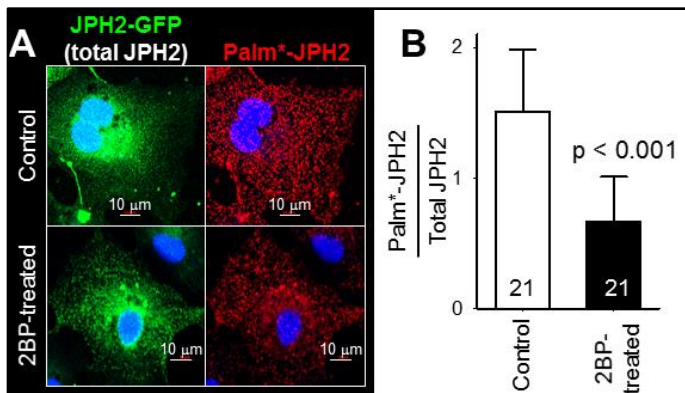


Fig. S2 Validating the Palm-PLA procedure for detecting palm*-JPH2. COS-7 cells expressing JPH2-GFP were incubated with palmitate-alkyne alone (control), or together with 2-bromopalmitate (2BP, palmitoylation inhibitor), both at 100 μ M, overnight. The cells were processed for Palm-PLA detected by red fluorophore. *Left*: Confocal images of JPH2-GFP (total JPH2) and palm*-JPH2 in control (top row) and 2BP-treated (bottom row) cells. We used the ratio of red fluorescence (palm*-JPH2) to green fluorescence (total JPH2) in each cell as a measure of relative degree of JPH2-GFP palmitoylation. *Right*: Data summary from 21 cells in each group. 2BP treatment reduced the degree of JPH2 palmitoylation by 50%.

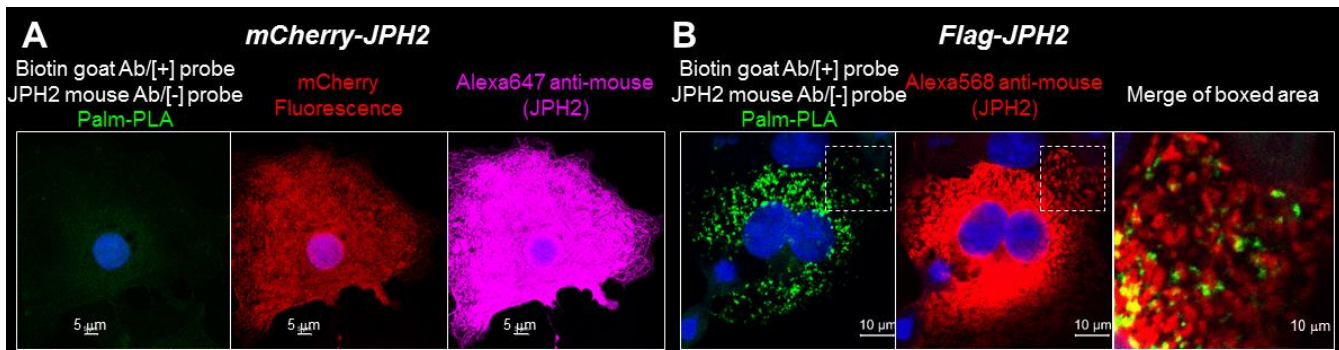


Fig. S3 Comparing the degree of palmitoylation between mCherry-JPH2 and flag-JPH2 using Palm-PLA. The same batch of COS-7 cells expressing mCherry-JPH2 (A) or flag-JPH2 (B) were subject to Palm-PLA using the same set of reagents on the same day. There was no Palm-PLA signal from mCherry-JPH2 despite clear mCherry fluorescence and JPH2 (Alexa647, far red) immunofluorescence, confirming strong expression of mCherry-JPH2. Strong signals of Palm-PLA with flag-JPH2 confirmed the success of the Palm-PLA reaction. These data corroborate Fig. 1C and Fig. 3D, showing that fusing mCherry to the N-terminus of JPH2 interfered with JPH2 palmitoylation.

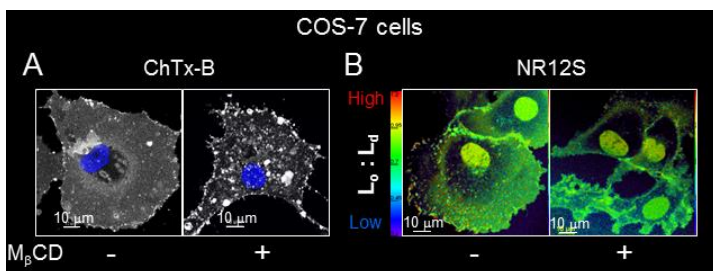


Fig. S4 Validating the efficacy of M β CD treatment (2 mM, 36°C, 2 hr) in disrupting lipid-raft and reducing liquid-ordered (L₀) subdomains in plasma membrane. **(A)** Live COS-7 cells labeled with Alexa488 Cholera toxin subunit B (ChTx-B), a lipid raft marker². M β CD treatment induced dramatic change in ChTx-B distribution pattern. **(B)** Live COS-7 cells labeled with Nile Red 12S (NR12S), a membrane lipid environment-sensitive fluorescent dye³. NR12S was excited by 514 nm laser and switching from liquid-ordered (L₀) to liquid-disordered (L_d) subdomains caused a red shift in its emission peak (from 570 to 605 nm). Shown are L₀:L_d ratio images of control and M β CD-treated cells, with color scale of L₀:L_d ratio shown on the left⁴. M β CD treatment reduced regions of high L₀:L_d ratio. We also used the total NR12S emission in the 523-581 nm and 591-698 nm ranges, defined as L₀ and L_d channels, to calculate the L₀:L_d ratio per cell. M β CD-treatment significantly reduced the normalized L₀:L_d value (from 1 ± 0.01 to 0.84 ± 0.01 , n=29 and 41, p<0.001), confirming a general decrease in the liquid-ordered subdomains in cell membranes. These data support the effectiveness of M β CD treatment in disrupting lipid raft subdomains, as was used in the experiments shown in Fig. 4A and 4B.

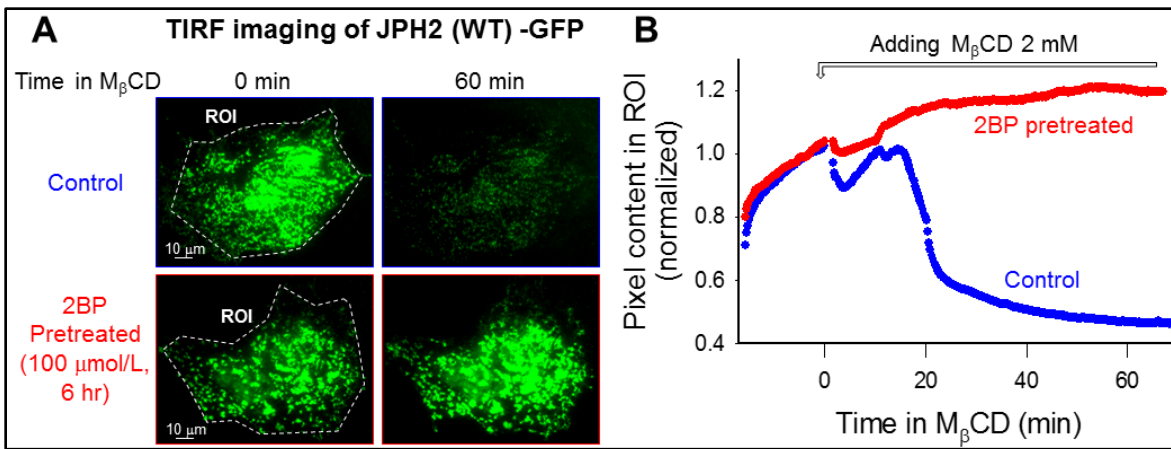


Fig. S5 Inhibiting palmitoylation by 2BP pretreatment prevents the suppressing effect of $M_{\beta}CD$ on juxtamembrane JPH2-GFP. COS-7 cells expressing JPH2-GFP were cultured under the control conditions or with 100 μ M 2BP before TIRF live cell imaging

experiments. **(A)** Images right before $M_{\beta}CD$ application and after 60 min in $M_{\beta}CD$. ROIs are marked. **(B)** Time courses of changes in pixel contents in ROIs (normalized to the initial pixel contents) from the same experiments as shown in (A). These data, in conjunction with those shown in Fig. 4C, suggest that palmitoylated JPH2 promoted or stabilized the formation of ER/PM junctions and enlarged the juxtamembrane JPH2 pools, which were sensitive to lipid-raft disruption by $M_{\beta}CD$ treatment. Preventing or reducing JPH2 palmitoylation (by replacing all four Cys by Ala or by 2BP pretreatment) reduced the juxtamembrane JPH2 pools, which were not sensitive to $M_{\beta}CD$ treatment.

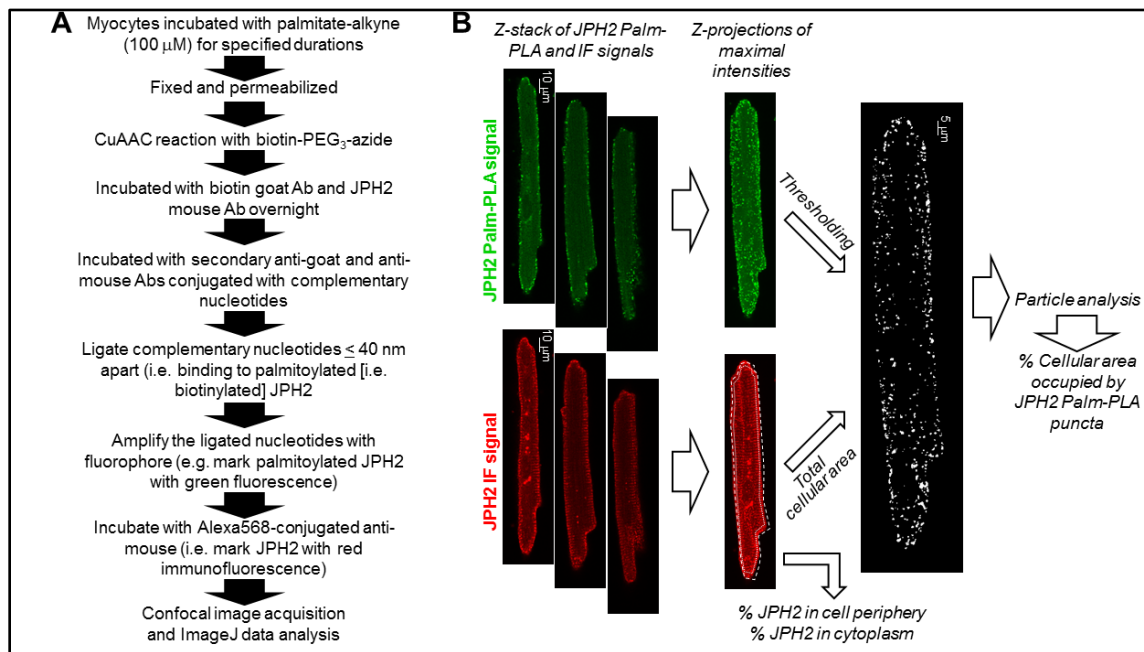


Fig. S6 Quantification of JPH2 Palm-PLA puncta using ImageJ. **(A)** Flow chart of experimental procedures to label palmitoylated and total JPH2 (by Palm-PLA and IF signals, respectively). **(B)** Image analysis with ImageJ. For each myocyte, z-stack images of Palm-PLA and JPH2 (IF) were collapsed into 2D images by z-projection of maximal intensity (Palm-PLA) or sum of intensities (JPH2 (IF)). The 2D image of Palm-PLA was thresholded to specify puncta, which were analyzed by ImageJ function: particle analysis. The total cellular area was determined from the JPH2 (IF) 2D image, and used to calculate the % cellular area occupied by JPH2 Palm-PLA puncta. Furthermore, the 2D image of JPH2 (IF) was used to calculate % JPH2 in cell periphery (2 μ m wide space between cellular contour delineated by the dash white lines, and the cytoplasm delineated by the dotted white lines).


```

JPH3      PKPRERRTESPVFTWTSHHRASNHSPGGSRLL--LELQEEKLSNYRMEMKPLLRMETHPQ      626
JPH4      -----ELAGYEADEAG--MQGGGP      525
          . * .

JPH1      VDVEDDGDGSSQSSSA-----L-----VHKPSAN--KWSPSKSVTKPVAKE-----      602
JPH2      FEDQPEPEVSGSESAPSSPATA--PLQAPTLRGPEFA--RETPAKLEPKPIIPK-----      630
JPH3      KRRYSKGGACRGLGDDHRPEDR--GFGVQLRSKAQNKENFRPASSAEPVQKLAASLR--      682
JPH4      RDGSPLLGGCSDSSGSLREEEGEDEEPLPLRA-----PAGTEPEPIAMLVLRGSS      576
          . . . : : * : :

          TMD
JPH1      -SKAEPKAKKSELA-IP-----KN--PASNDSCPALEKEANS GPNSIMIVLVMLLNIGL      652
JPH2      -AEPRAKARKTEARGLTKAGAKKKA--RKEAALAAEAEEVEEVPNTILICMIVLLNIGL      687
JPH3      LGGAEPRLLRWDL---TFSPQKSLPVALESDEENGDELKSTGSAPIILVVMVILLNIGV      739
JPH4      SRGPDAGGLTEEL-----GEPATERPAQPGAANPLVVGAVALLDLSL      619
          : . . : : * * * : :

JPH1      AILFVHFLT      661
JPH2      AILFVHLLT      696
JPH3      AILFINFLT      748
JPH4      AFLFSQLLT      628
          * : * * : :

```

E. Ranking of potential S-palmitoylation sites in JPH1-JPH4 using CSS-Palm 4.0
(<http://csspalm.biocuckoo.org/online.php>)

Domain location	JPH1		JPH2		JPH3		JPH4	
	Position	Score	Position	Score	Position	Score	Position	Score
MORN 1	C15	9.283	C15	9.506	C16	8.821	C14	7.256
MORN 1	C29	0.384	C29	0.364	C30	0.838	C30	0.679
MRON 2							C42	4.694
Between MORN 5-6	C101	1.213			C100	0.618		
After MORN 6	C264	0.901						
MORN 6	C267	3.071						
MORN 8	C318	7.363	C328	4.482	C325	4.853		
Helix	C402	0.418						
Coil					C441	3.753	C476	8.582
					C526	3.854	C535	6.654
					C636	1.156		
TMD	C626	8.025	C678	6.314			C584	4.94